International Journal of Modern Physics A
Vol. 37, No. 7 (2022) 2240017 (13 pages)

DOI: 10.1142/S0217751X22400176

The ENUBET experiment

C. C. Delogu,[*,†,‡‡‡‡] F. Acerbi,[‡,§] A. Berra,[¶,‖] M. Bonesini,[‖] A. Branca,[*,†] C. Brizzolari,[‖,**] G. Brunetti,[‖] M. Calviani,[††] S. Capelli,[¶,‖] S. Carturan,[‡‡] M. G. Catanesi,[§§] S. Cecchini,[¶¶] N. Charitonidis,[††] F. Cindolo,[¶¶] G. Collazuol,[*,†] E. Conti,[†] F. Dal Corso,[†] G. De Rosa,[‖‖] A. Falcone,[‖,**] A. Gola,[‡,§] F. Iacob,[*,†] C. Jollet,[***,†††] V. Kain,[††] B. Kliček,[‡‡‡] Y. Kudenko,[§§§] M. Laveder,[*,†] A. Longhin,[*,†] L. Ludovici,[¶¶¶] E. Lutsenko,[¶,‖] L. Magaletti,[§§] G. Mandrioli,[¶¶] A. Margotti,[¶¶] V. Mascagna,[¶,‖] N. Mauri,[¶¶] L. Meazza,[‖,**] A. Meregaglia,[†††] M. Mezzetto,[†] M. Nessi,[††] A. Paoloni,[‖‖‖] M. Pari,[*,†] E. G. Parozzi,[‖,**] L. Pasqualini,[¶¶,****] G. Paternoster,[‡,§] L. Patrizii,[¶¶] M. Pozzato,[¶¶] M. Prest,[¶,‖] F. Pupilli,[†] E. Radicioni,[§§] C. Riccio,[‖‖,††††] A. C. Ruggeri,[‖‖] C. Scian,[*] G. Sirri,[¶¶] M. Stipčević,[‡‡‡] M. Tenti,[¶¶] F. Terranova,[‖,**] M. Torti,[‖,**] E. Vallazza,[‖] F. Velotti[††] and L. Votano[‖‖‖]

[*] *Department of Physics, Università di Padova, Via Marzolo 8, Padova, Italy*

[†] *INFN Sezione di Padova, Via Marzolo 8, Padova, Italy*

[‡] *Fondazione Bruno Kessler (FBK), Trento, Italy*

[§] *INFN TIFPA, Trento, Italy*

[¶] *Dipartimento di Scienza e Alta Tecnologia (DiSAT), Università degli Studi dell'Insubria, Via Valleggio 11, Como, Italy*

[‖] *INFN, Sezione di Milano-Bicocca, Piazza della Scienza 3, Milano, Italy*

[**] *Physics Department, Università di Milano-Bicocca, Piazza della Scienza 3, Milano, Italy*

[††] *CERN, Geneva, Switzerland*

[‡‡] *INFN, Laboratori Nazionali di Legnaro, Viale dell'Università, 2, Legnaro, PD, Italy*

[§§] *INFN Sezione di Bari, Via Amendola 173, Bari, Italy*

[¶¶] *INFN, Sezione di Bologna, Viale Berti-Pichat 6/2, Bologna, Italy*

[‖‖] *INFN, Sezione di Napoli, Via Cinthia, 80126 Napoli, Italy*

[***] *Institut Pluridisciplinaire Hubert Curien (IPHC), CNRS/IN2P3, Université de Strasbourg, Strasbourg, France*

[†††] *Centre de Etudes Nucléaires de Bordeaux Gradignan, 19 Chemin du Solarium, Bordeaux, France*

[‡‡‡] *Center of Excellence for Advanced Materials and Sensing Devices, Ruder Bošković Institute, HR-10000 Zagreb, Croatia*

[‡‡‡‡] Corresponding author.

§§§ *Institute of Nuclear Research, Russian Academy of Science, Moscow, Russia*

¶¶¶ *INFN, Sezione di Roma 1, Piazzale Aldo Moro 2, Rome, Italy*

‖‖‖ *INFN, Laboratori Nazionali di Frascati, Via Fermi 40, Frascati (Rome), Italy*

**** *Physics Department, Università di Bologna, Viale Berti-Pichat 6/2, Bologna, Italy*

†††† *Physics Department, Università degli Studi di Napoli Federico II, Via Cinthia, 80126 Napoli, Italy*

‡‡‡‡ *claudiacaterina.delogu@pd.infn.it*

Received 31 March 2021
Accepted 26 December 2021
Published 3 March 2022

The knowledge of the initial flux in conventional neutrino beams represents the main limitation for a precision (1%) measurement of ν_e and ν_μ cross-sections. The ENUBET ERC project is studying a facility based on a narrow-band beam capable of constraining the neutrino fluxes normalization through the monitoring of the associated charged leptons in an instrumented decay tunnel. In particular, the identification of large-angle positrons from K_{e3} decays at single-particle level can reduce the ν_e flux uncertainty at the level of 1%. This setup would allow for an unprecedented measurement of the ν_e cross-section at the GeV scale. Such an experimental input would be highly beneficial to reduce the budget of systematic uncertainties in the next long baseline oscillation experiments. The ENUBET Collaboration presented at ICNFP 2020 the advances in the design and simulation of the hadron beamline, the optimization and performances of a 20 m long focusing transfer line, the design of an horn-based beamline, the results in terms of particle identification in the decay tunnel, and the final design of the ENUBET demonstrator for the instrumented decay tunnel.

Keywords: Neutrino; neutrino beams.

1. ENUBET: Enhanced NeUtrino BEams from Kaon Tagging

In the near future, neutrino physics will require measurements of absolute neutrino cross-sections at the GeV scale with 1% precision. Modern cross-section experiments are reaching the intrinsic limitations of conventional neutrino beams: ν_e and ν_μ fluxes are inferred by a full simulation of meson production and transport from the target down to the beam dump and are validated by external data and, hence, neutrino fluxes are affected by significant uncertainties, of the order of 5–10%. ENUBET is an ERC project (2016–2021, p.i. Andrea Longhin). Since March 2019 it is also part of the CERN Neutrino Platform as NP06/ENUBET. The ENUBET experiment aims at demonstrating the feasibility of a monitored neutrino beam, in which the absolute normalization of the neutrino flux produced by a narrow-band beam can be constrained at the 1% level. The goal is to study a facility where the electron neutrino component from K_{e3} decays ($K^+ \to e^+\pi^0\nu_e$) can be monitored on a single-particle level by instrumenting a fraction of the decay region: the "tagger".

The electron neutrino flux is monitored by the observation of large-angle positrons in the decay tunnel.[1]

The two main pillars of the project are the design of the π/K focusing and transport system, with suitable proton extraction schemes, to keep the rate of particles in the tunnel at a level sustainable for the tunnel instrumentation, and the construction of a detector capable of performing positron identification in the decay tunnel at single-particle level.

ENUBET[2,3] will consist in a conventional narrow-band beam with a short (20 m) transfer line followed by a 40 m long decay tunnel. After the proton beam is extracted and directed toward the target, secondary hadrons are momentum and sign selected and transported to the decay pipe. The secondary beam is designed to have an average momentum of 8.5 GeV and a $\pm 10\%$ momentum bite. Noninteracting protons are stopped in a beam dump. Off-momentum particles reaching the decay tunnel are mostly low-energy pions, electrons, positrons and photons coming from interactions in other beamline components, and muons from pion decay that cross absorbers and collimators (see Sec. 2). Particle creation in the decay tunnel can be monitored at single-particle level by calorimetric techniques (see Sec. 3). The measurement of muons in the tagger and after the hadron dump allows to determine the ν_μ flux from kaons and pions, respectively. In addition, in a narrow-band beam, the transverse position of the neutrino interaction at the detector can be exploited to determine *a priori*, with significant precision, the neutrino energy spectrum without relying on the final state reconstruction. Particles identification is performed by a Neural Network (NN) approach based on a Multivariate Data Analysis (described in Sec. 4).

Finally, different prototypes were built and tested at CERN PS East Area in order to select the appropriate layout for the tagger demonstrator: the first prototypes were shashlik calorimeters while the last one was built with lateral scintillation light readout. This will be discussed in Sec. 3.

2. The ENUBET Beamline

After the original ENUBET proposal,[1] the collaboration has developed a complete simulation of the beamline, re-optimized the beam parameters and studied additional backgrounds coming from beam halo. The development of the ENUBET beamline is performed taking into account different factors[2,4]:

- maximize the number of K^+ in the momentum range of interest at tunnel entrance;
- minimize the total length of the transfer line ($\sim$20 m) to reduce kaon decay losses before the entrance of the decay tunnel;
- produce a small beam size: nondecaying particles should exit the decay pipe without hitting the tagger inner surface;
- keep under control the level of background transported to the tunnel, which affects the signal-to-noise (S/N) ratio of the positron selection;

Table 1. Expected rates of π^+ and K^+ for proton on target (PoT) in $6.5 \div 10.5$ GeV range at the decay tunnel entrance for the two possible focusing schemes. The improvement factor in kaon transport with respect to proposal[1] is shown in the last column.

Focusing system	π^+/PoT (10^{-3})	K^+/PoT (10^{-3})	Extraction length	π/cycle (10^{10})	K/cycle (10^{10})	Factor with respect to Ref. 1
Horn-based	77	7.9	2–10 ms	438	36	$\times 2$
Static	19	1.4	2 s	85	6.2	$\times 4$

- use of conventional magnet field and apertures (normal-conducting devices, with an aperture below 40 cm).

The optics is currently optimized for a reference hadron beam with a momentum of 8.5 GeV/c and a momentum bite of 10%.

Two possible beamlines[5] have been considered: the "horn-based transfer line" features a focusing horn placed between the ENUBET target and the following transfer line, while in the "static transfer line" the transfer line quadrupoles are placed directly downstream the target. Horn-based transfer line studies are being pursued due to the remarkable fluxes that can be achieved. On the other hand, the performances of the static design (see Subsec. 2.1), as shown in Table 1, turned out to be better than early estimates reported in the ENUBET proposal[1] and allows to perform the focusing using DC operated devices, offering several advantages in terms of costs and technical implementation.

2.1. *The "static" focusing transfer line*

One advantage with respect to a horn-based line is that there are no intrinsic time limits for proton extractions, up to several seconds. Consequently, the particle rate at the tunnel instrumentation could be reduced, reducing pile-up effects. The single resonant slow extraction (2 s) is less challenging than a horn-based beamline. An additional advantage is the possible determination of the ν_μ flux through a direct monitoring of the muon rate after the hadron dump, from π^+ and K^+ decays (see Subsec. 4.1).

The secondary particles production from primary proton interactions with the target is simulated with FLUKA. The results presented are based on primary protons with momenta of 400 GeV on a Carbon target. The estimation of the doses in the decay tunnel is addressed using FLUKA. The tagger calorimeter has been surrounded by a layer of Borated Polyethylene, leading to a reduction of neutron fluences.

The optimization of the magnetic lattice of the beamline (dipoles and quadrupoles) is performed with TRANSPORT. A full simulation of particle transport and interaction is performed with G4beamline. The same setup has also been implemented in GEANT4, this modeling is useful for the study of systematic uncertainties.

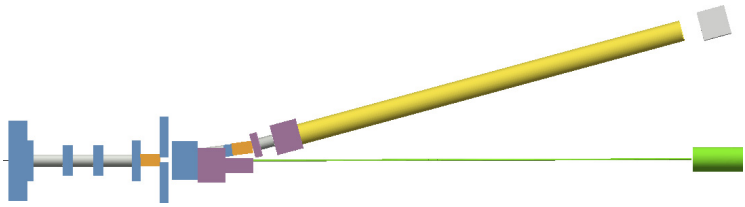

Fig. 1. Schematics of the ENUBET double dipole beamline, static focusing option.

The transfer line is ∼20 m long. The quadrupole-based focusing system is designed to be operated with a slow extraction proton scheme, where protons can be diluted over several seconds.

The best configuration achieved (Fig. 1) consists of quadrupole triplet followed by a bending dipole, a correction quadrupole, a second bending dipole and one last quadrupole. The dipole field provides a bending angle of 7.4° for each dipole, for a total bending of the secondary beam of 14.8° with respect to the primary beam. This configuration is still under optimization.

This design features a larger overall bending angle with respect to the original proposal (single dipole beamline[2,6]). The length of this transfer line is greater than the single dipole option, but significant advantages of this design are a better collimated beam, and a reduction of the beam halo background (in particular from muons) and of the untagged neutrino component at the far detector: neutrinos produced in the straight section of the transfer line have a lower probability to reach the detector (more details in Subsec. 2.3).

The optimization concerns also collimators and shielding. In particular, a Tungsten foil after the target dumps low-energy positrons entering the decay pipe. We studied different options for an Inermet180 block to be placed before in front of the decay pipe, in order to reduce the background of particles hitting the calorimeter walls.

Figure 2 shows the expected beam composition at the tagger entrance, Fig. 3 shows the spectra of π^+ and K^+ entering/exiting the decay tunnel.

2.2. *The horn-based transfer line — "burst slow extraction"*

The reduced meson yield of the longer double dipole beamline, and hence the neutrino flux reduction, is compensated in this option by a horn-based focusing, paired with a "burst slow extraction" that has been recently demonstrated experimentally at CERN-SPS in the context of the ENUBET machine studies.

This transfer line features a magnetic horn placed between the target and the quadrupoles. We need a dedicated proton extraction scheme with $\mathcal{O}$(ms) long spills in order to not exceed the tolerable particle rate in the tagger and the maximum current pulse duration for the magnetic horn. The proton spill would be extracted in bursts of 2–10 ms, repeated with a frequency of 10 Hz during the flat top of the

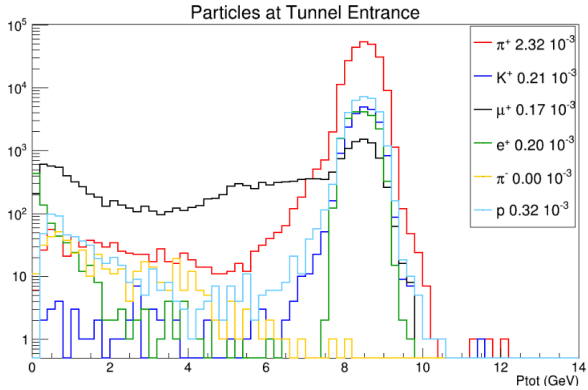

Fig. 2. Particle budget at tagger entrance, normalized to PoT.

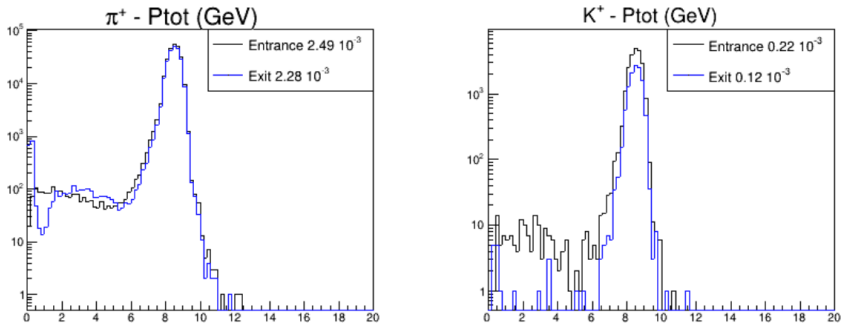

Fig. 3. (Color online) Momentum distribution of π^+ (left) and K^+ (right) at tagger entrance (black)/exit (blue).

accelerator. This "burst slow extraction" has been successfully implemented at the SPS, obtaining pulse lengths of 20 ms (Fig. 4).

Dedicated simulation studies showed the possibility to obtain a 2–10 ms range, and they will be validated after LS2.

2.3. *Flux components*

The double-dipole "static" focusing transfer line (Subsec. 2.1) is beneficial to reduce the untagged neutrino component at the far detector. With the assumption of a 500 t neutrino detector located 50 m from the decay tunnel, 10^4 ν_e^{CC} will be observed at the detector in about 1.5 yr of data taking.

Figure 5 shows the ν_e^{CC} spectra at the far detector, divided in categories depending on the position of the neutrino production along the beamline. Eighty percent of these events are directly monitored, which means that are created in the decay tunnel. Ten percent low-energy events come from early decays or interactions of kaons, they are removable with an energy cut. Ten percent of the flux is given by decay in the transfer line straight section in front of the tagger, pointing to the detector

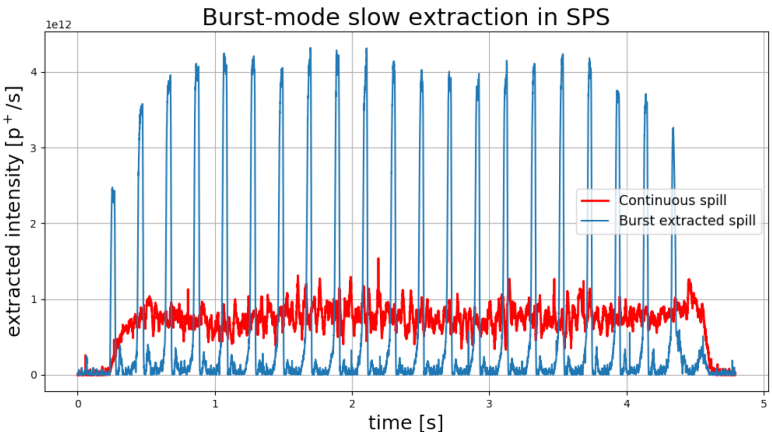

Fig. 4. Burst slow extraction over an SPS spill, compared to the standard slow extracted spill.[7]

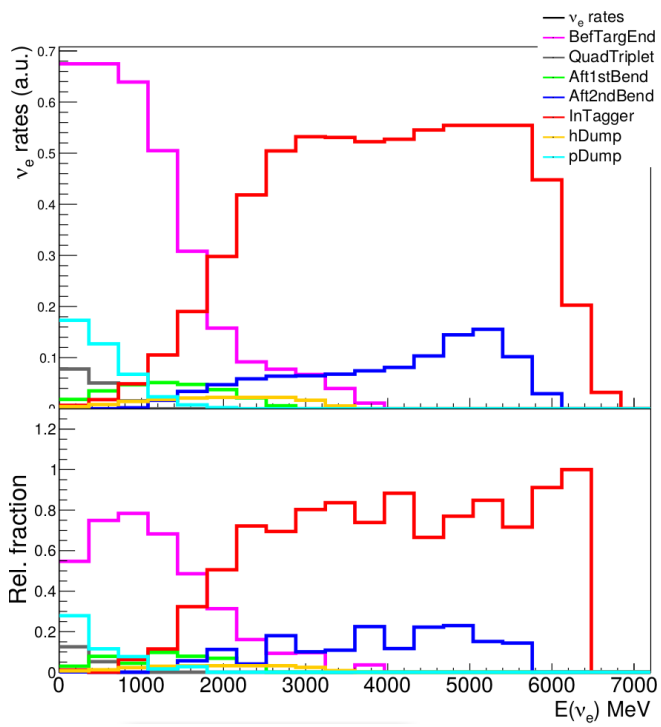

Fig. 5. ν_e^{CC} interactions divided in categories, corresponding to the position of the neutrino production along the beamline.

(i.e. from the second dipole to the tagger entrance, see Fig. 1 for the schematic of the beamline). These events are removable with the simulation.

3. Decay Tunnel Instrumentation: The Positron Tagger

The ENUBET positron tagger consists of a calorimeter for e/π separation and of an inner detector for e/π^0 separation and timing ("t_0-layer").[1] In the baseline design it is a cylinder surrounding a fraction of the decay tunnel. The requirements for the detector are:

- high e/π separation capability to remove the main source of background;
- radiation hardness;
- cost effectiveness, since a large fraction of the decay tunnel will be instrumented;
- fast recovery time, in order to cope with the expected rate of 200 kHz/cm^2.

These requirements are fulfilled by a sampling calorimeter with longitudinal segmentation for positron tagging, complemented by a photon veto.

The light readout system is based on WaveLength Shifting (WLS) fibers, used for the light collection, and Silicon PhotoMultipliers (SiPMs).

The building block of the ENUBET tagger is the Ultra Compact Module (UCM). The first prototypes tested were shashlik calorimeters[8–10] (sampling calorimeters in which the tiles of absorbing and scintillating materials are crossed perpendicularly by the WLS fibers) with dimensions of $10 \times 3 \times 3$ cm^3, that cover 4.3 X_0 and 1.7 Moliere radii. This segmentation allows to separate positrons from charged pions with a misidentification probability lower than 3%.

The integration of the light readout into the calorimeter module results in exposing the SiPMs to fast neutrons produced by hadronic showers. The effect of the radiation on the performances of the SiPMs was evaluated in Ref. 11.

The current design (see Subsec. 3.1) is based on a new prototype that provides reduction of neutron damage risk. It consists in a scheme where light is collected from the sides of the scintillator tiles, replacing the UCM with a Lateral readout Compact Module (LCM).

The final layout of the tagger will be composed by three calorimeter layers of LCMs, and equipped with the photon veto (described in Subsec. 3.2).

3.1. *Lateral light readout prototype*

Each LCM unit consists of a stack of five $3 \times 3 \times 1.5$ cm^3 iron tiles interleaved with five $3 \times 3 \times 0.5$ cm^3 plastic scintillator tiles. Ten WLS fibers, placed at both sides of each scintillator tile, carry the light to a SiPM placed on top of the calorimeter, at a distance of about 30 cm, as in Fig. 6, above a Borated Polyethylene shield. FLUKA simulations demonstrated[12] that there is a reduction of a factor 18 placing SiPMs above this layer.

In 2018[12] a prototype made of $3 \times 2 \times 2$ LCM was tested at CERN PS East Area. Later two additional blocks of LCMs have been developed, using the same

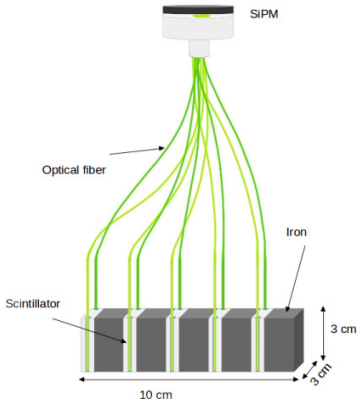

Fig. 6. Schematics of one LCM.

Fig. 7. Lateral readout prototype tested in 2018, with integrated photon veto (bottom right).

techniques, resulting in a $7 \times 4 \times 3$ LCM calorimeter as shown in Fig. 7. The planes of LCMS were shifted with respect to each other, because of the extraction of the WLS fibers: they must be coupled only to one scintillator tile, without collecting light from the above plane. For the same reason, iron tiles are grooved on both sides in order to allow the passage of the fibers.

During the testbeam the calorimeter was tilted at different angles (0, 50, 100, 200 mrad) with respect to the beam direction, to reproduce the ENUBET particle flow, and exposed to a mixed beam of electrons, pions and muons.

The calorimeter response to minimum ionizing particles (mips'), electrons and pions was evaluated and showed a good agreement with the prediction of a Monte Carlo simulations, in the 1–3 GeV range. Testbeam results showed an electromagnetic energy resolution at 1 GeV of about 17% (Fig. 8) and a linear response in the range 1–3 GeV, consistent with the prediction.

3.2. *The photon veto*

Discrimination of photons from π^0 decay ($\pi^0 \to \gamma\gamma$) can be reached by employing an integrated photon veto: a thin plastic scintillator ring installed below the inner

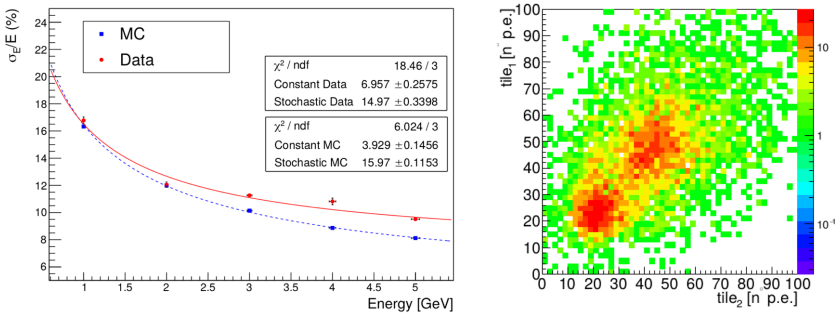

(a) (b)

Fig. 8. (Color online) Results from the 2018 testbeam. (a) Electromagnetic energy resolution versus beam energy for particles impinging on the front face of the calorimeter, for data (red dots) and simulation (blue squares). Points are fitted with $\frac{\sigma_E}{E} = \frac{S}{\sqrt{E}} \oplus C$, where S and C are, respectively, the stochastic and constant term. (b) Number of photoelectrons collected in one t_0 tile versus the other. The two peaks corresponding to 1 and 2 mip distributions are discernible.

radius of the calorimeter ("t_0-layer") allows π^0 rejection. The basic unit is a doublet of plastic scintillator tiles, each tile ($3 \times 3 \times 0.5$ cm^3) is readout by two lateral WLS fibers linked to a single SiPM. Photon conversions are discriminated from positrons using the information on the pulse height in all hit scintillators. Photon converted in the photon veto are rejected requiring a signal compatible with a single mip (1–2 mip separation, Fig. 8(b)). During the 2018 testbeam[12] the t_0-layers were tested coupled with the calorimeter, in terms of mip response, timing resolution and light collection efficiency.

3.3. *The ENUBET demonstrator*

The final design of the ENUBET demonstrator for the instrumented decay tunnel has been selected on the basis of the results of the 2016–2018 testbeams. This large detector prototype will prove the scalability and performance of the selected detector technology: an iron-scintillator sampling calorimeter (for e/π separation) with a lateral light readout (as seen in Subsec. 3.1) through WLS fibers connected to SiPMs, coupled with a photon veto (for e/π^0 separation) made by an inner ring of plastic scintillator trackers. In this layout the interference between WLS fibers in different radial layers is avoided by employing frontal readout (light collection) and transit (hosting fibers from previous layers) grooves (see Fig. 9). The difference in response in light collection depending on the position of the WLS fibers in the scintillator was studied with GEANT4.

4. Particle Reconstruction

The instrumentation of the ENUBET decay pipe has been implemented in a GEANT4 simulation, in order to test the particle identification (PID) performance

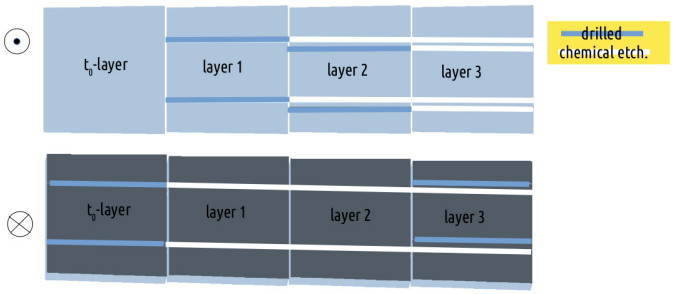

Fig. 9. The ENUBET demonstrator will consist in three radial layers of LCMs, coupled with an inner ring of photon veto. The frontal grooves on the scintillator tiles are organized such that the readout grooves of different layers are shifted with respect to each other. The transit grooves will be treated in order to make them optically opaque.

of the tagger.[13] Secondary mesons are generated at the tunnel entrance starting from particles transported by the beamline (see Subsec. 2.1) to this point. The response of the tagger is simulated at hit level, not considering the scintillation process and light propagation. A waveform simulation, based on the SiPM response, is being developed in order to include the pile-up effect.

PID is based on a Multivariate Data Analysis that employs variables constructed from the energy deposit in each module of the calorimeter. PID starts from an event seed associated to a large energy deposit. The first step needed for PID is the definition of the event by the ENUBET Event Builder (EB).

The EB identifies the "seed" of the event: the LCM with an energy deposition in inner layer exceeding 28 MeV is selected as seed for the event reconstruction.[a] Neighbor LCMs and t_0 signals correlated to the seed are clustered, taking into account their position and timing. The procedure is iterated over all the signals recorded.

Once the event has been defined, PID is based on the calorimetric capabilities of the detector, as well as on the information coming from the t_0-layer. We used a NN based on Toolkit for Multivariate Data Analysis (TMVA) multivariate analysis. Charged particles will deposit energy in different modules and the NN relies on the pattern of energy deposition in the calorimeter through a set of 19 variables (energy pattern deposition in calorimeter, event topology and photon-veto energy deposition).

Positrons are selected with an efficiency of 24% and a S/N ratio of 2.1. Figure 10 shows the distributions of the total visible energy, one of the relevant observables, after the event building and after the NN discrimination.

[a]The energy released by a single mip in a LCM is about 6.5 MeV.

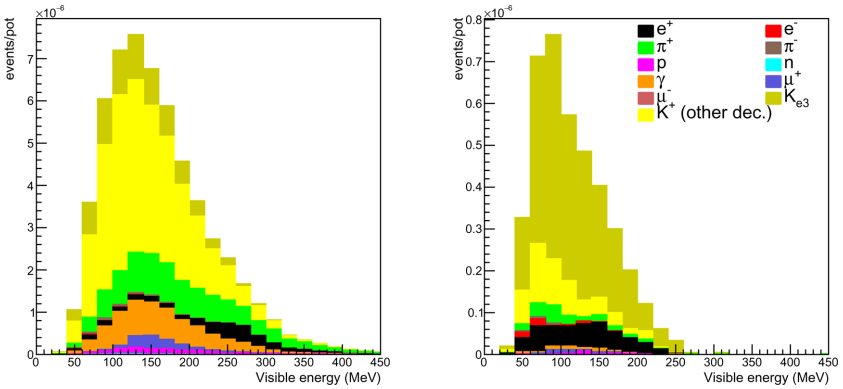

Fig. 10. Total visible energy after the event building (left) and after applying the NN cut (right).

4.1. *Muon monitoring*

The sensitivity of the ENUBET experiment can be extended monitoring the muon neutrino component, from the decays of K^+ and π^+. The two contributions are separated in energy: in the ENUBET narrow-band beam the ν_μ from kaon/pion decays represent the high-/low-energy component. The tagger calorimeter constrains the high-energy neutrinos, since the associated large angle muons are in its acceptance region, while the low-energy neutrinos from pion decays are collinear with the beamline and could be constrained by "muon stations" placed after the hadron dump. The preliminary design of this detector consists in alternated planes of absorbers and detectors. The choice of detector technology and the estimation of muon rate is under study.

A dedicated EB has been implemented to reconstruct muons from $K^+ \to \mu^+\nu_\mu$ and $K^+ \to \pi^0\mu^+\nu_\mu$ kaon decays. It identifies the inner layer LCM with energy between 5 and 15 MeV as the seed of the event, and all LCM deposits compatible with muon-track topology and propagation are clustered to build the event. The μ-like background separation is performed by a TMVA exploiting 13 variables (energy deposition, track isolation and topology)

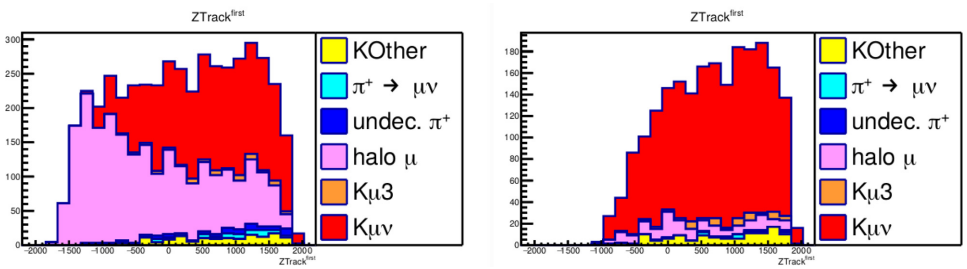

Fig. 11. Impact point along the tagger for muons from kaon decays, before (left) and after (right) applying the NN cut.

This analysis chain allows to select muons with an efficiency of 35%/21% for the two-/three-body decay, and a S/N of 6.1. Figure 11 shows the distributions of the impact point along the tagger for muons from kaon decays.

5. Conclusions

From the start of the project in 2016, ENUBET has achieved important results and has extended its physics potential.

The R&D includes the design and simulation of the beamline: the feasibility of a purely static focusing system, and the test of the burst slow extraction scheme at the CERN-SPS are the major highlights. Lepton identification at single-particle level has been achieved for the static focusing system with very good performance. Finally, testbeams campaigns for the test of the tagger prototypes have been completed at the CERN East Area before LS2.

The ongoing studies concern the horn optimization, the update of flux and spectra with the final beamline, and the establishment of the final systematic budget. We plan to complete the construction of the demonstrator and to set up a framework for the full assessment of systematics by the end of 2021, and to complete the test of the demonstrator by the end of 2022.

Acknowledgment

This project has received funding from the European Research Council (ERC) under the European Unions Horizon 2020 research and innovation program (Grant Agreement 681647).

References

1. A. Longhin, L. Ludovici and F. Terranova, *Eur. Phys. J. C* **75**, 155 (2015).
2. F. Acerbi *et al.*, arXiv:1901.04768 [physics.ins-det].
3. F. Terranova *et al.*, *PoS* **NuFact2019**, 121 (2020).
4. A. Berra *et al.*, Enabling precise measurements of flux in accelerator neutrino beams: The ENUBET project, CERN-SPSC-2016-036, SPSC-EOI-014.
5. F. Acerbi *et al.*, The ENUBET project, CERN-SPSC-2018-034. SPSC-I-248.
6. G. Brunetti *et al.*, *PoS* **EPS-HEP2019**, 387 (2020).
7. M. Pari, M. Fraser, B. Goddard, V. Kain, L. Stoel and F. Velotti, Model and measurements of CERN-SPS slow extraction spill re-shaping — The burst mode slow extraction, in *Proc. 10th Int. Particle Accelerator Conf.* (*IPAC'19*), Melbourne, Australia, 2019, p. 2406.
8. A. Berra *et al.*, *Nucl. Instrum. Methods A* **830**, 345 (2016).
9. A. Berra *et al.*, *IEEE Trans. Nucl. Sci.* **64**, 1056 (2017).
10. F. Acerbi *et al.*, *Nucl. Instrum. Methods A* **956**, 163379 (2020).
11. F. Acerbi *et al.*, *J. Instrum.* **14**, P02029 (2019).
12. F. Acerbi *et al.*, *J. Instrum.* **15**, P08001 (2020).
13. F. Pupilli *et al.*, *PoS* **NEUTEL2017**, 078 (2018).